# CHARACTERIZATION AND SIMULATION OF MULTICRYSTALLINE LLC-SI THIN FILM SOLAR CELLS

G. Andrä[1], J. Bergmann[1], A. Bochmann[1], F. Falk[1], E. Ose[1], S. Dauwe[2], T. Kieliba[3]

[1]Institut für Physikalische Hochtechnologie, Albert-Einstein-Str. 9, D-07745 Jena, Germany,
email: falk@ipht-jena.de

[2]CiS Institut für Mikrosensorik gGmbH, SolarZentrum Erfurt, Konrad-Zuse-Str. 14, D-99099 Erfurt, Germany,
email: sdauwe@cismst.de

[3]ErSol Solar Energy AG, Wilhelm-Wolff-Str. 23, D-99099 Erfurt, Germany, email: thomas.kieliba@ersol.de

ABSTRACT: A multicrystalline silicon thin film solar cell on a low cost low temperature glass in the superstrate configuration prepared by Layered Laser Crystallization (LLC) is presented with crystallites in the 10 to 100 μm range throughout. The thickness of the p-doped absorber is varied between 2 and 5 μm. The highest value for the short circuit current of 19 mA/cm² was achieved for 5 μm absorber cells whereas the highest value of open circuit voltage occurred for 2 μm absorber cells. The highest efficiency reached so far is 4.8%. Cell simulations agree with the measured cell data if recombination parameters are adjusted properly.
Keywords: Silicon, Thin Films, Laser Processing

## 1 INTRODUCTION

As an alternative to mono or multicrystalline silicon bulk solar cells in the last years crystalline silicon thin film cells have received growing interest due to economic reasons. Typical examples are microcrystalline cells deposited under specific CVD conditions [1,2], quasi-monocrystalline thin film cells prepared by a transfer process from the surface of a wafer onto a glass substrate [3,4], or multicrystalline cells based on layers produced by aluminum induced crystallization [5].

Another alternative are multicrystalline silicon thin film cells prepared by the LLC (Layered Laser Crystallization) technology [6,7], which, in contrast to the process used for quasi-monocrystalline cells, is well suited for large area processing. As compared to the direct deposition of microcrystalline silicon, the LLC technology has the potential for high deposition rates. LLC cells do not contain, in contrast to cells based on aluminum induced crystallization, microcrystalline regions which reduce the cell performance appreciably.

In this paper the LLC technology for preparing multicrystalline silicon thin film cells consisting of 100 μm wide crystallites on a low cost glass substrate is presented. The properties of LLC cells are reported and compared with results of cell simulations.

## 2 EXPERIMENTAL

The multicrystalline LLC cell as shown in Fig. 1 is prepared on a borosilicate glass substrate (Schott borofloat 33 or Corning 7059). The LLC process, described in detail in [6,7], is as follows.

First 700 nm of a-Si are deposited by a conventional PECVD process at 13.56 MHz from silane diluted in He at a substrate temperature slightly above the annealing point of the glass substrate (590 or 560°C). 0.1% to 0.2% diborane is added to silane for heavy p doping ($5 \times 10^{19}$ cm$^{-3}$ boron). This layer is crystallized in the deposition chamber by scanning the gaussian beam of an Ar$^+$- or frequency doubled Nd:YAG-laser with a center intensity of 25 kW/cm² at a rate of 5 cm/s. The beam is scanned in rows overlapping by 50 to 60%. In this way a seed layer consisting of crystallites 10 to 100 μm in size is prepared which, in addition, acts as one of the electrodes.
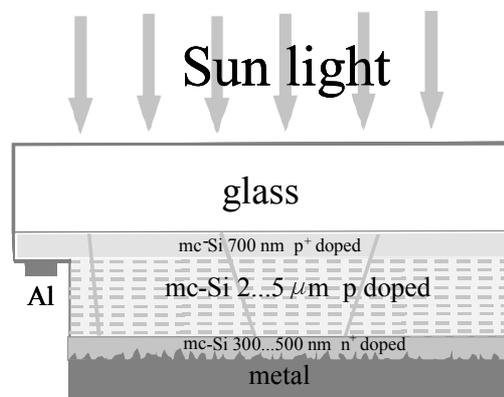


**Figure 1**: Design of the LLC cell

Onto the seed layer further a-Si:H is deposited in the same chamber to prepare the absorber. The diborane concentration in silane is reduced to 3 to 10 ppm resulting in a boron concentration of $5 \times 10^{16}$ to $5 \times 10^{17}$ cm$^{-3}$. There is no break in deposition between seed layer crystallization and this step. During the deposition pulses of a KrF excimer laser (248 nm wavelength, 25 ns pulse duration) are applied in regular intervals whenever 20 to 80 nm a-Si have been deposited. The laser beam has, after passing a homogenizer, a square cross section of 6x6 mm² and a fluence of 550 to 800 mJ/cm². Each laser pulse leads to melting of the newly deposited a-Si and of a thin layer of multicrystalline Si below. After the pulse, vertical epitaxial growth starts from the multicrystalline Si reproducing the 100 μm grains of the seed into the absorber. This procedure is continued until the desired absorber thickness of 2 to 5 μm is reached.

Areas larger than the cross section of the excimer laser beam can be crystallized, if the beam is translated laterally so that slightly overlapping patches are irradiated sequentially.

After absorber growth a 300 to 500 nm thick n-doped emitter is prepared without interruption. The diborane flux is stopped and 0.3% phosphine are introduced instead resulting in a phosphorus concentration of $5 \times 10^{19}$ cm$^{-3}$. Application of excimer laser irradiation is continued yielding epitaxial growth after melting as during absorber preparation. Therefore the emitter has the same crystal structure as absorber and seed layer.

Finally the silicon layers are passivated by a micro-wave remote plasma hydrogen treatment (0.25 hPa total pressure, 40 sccm $H_2$, 4 sccm Ar for 30 min. at 400 to 450 °C).

After preparation of the silicon layer system a structuring step follows. On the layer system an etching mask is prepared by photolithography. By a chemical etching step down to the highly p-doped seed layer cells 1 to 12 mm² in area are prepared.

For contacting aluminum is deposited onto the free areas of the seed layer by evaporation through a mask.

Finally Al, Ag, or TiPdAg back contacts are deposited by evaporation through a mask. In addition, this metal layer serves as a back reflector.

For diagnostics the metal electrode layer sometimes was omitted and the cell was contacted by metal tips instead.

With respect to the crystal structure the cells were characterized by TEM and EBSD (electron beam back scatter diffraction). For measuring I-V-curves the cells were illuminated by a AM1.5 spectrum sun simulator (PET model SS 80). The carrier lifetime was measured by MWPCD (microwave photoconductance decay) [8] and by QSSPC (quasi-steady state photoconductance) [9]. Based on parameters extracted from these measurements 1-d cell simulations were performed using the program PC1D [10].

3   RESULTS

Thin film cells 2x2 cm² in size with 2 to 5 µm thick absorber layers were prepared by the LLC technology (Fig. 2). The layer system consists of crystallites with a lateral size of 10 to 100 µm (Fig. 3). These crystallites extend from substrate to top as was verified by TEM (Fig. 4) and EBSD. The TEM image demonstrates that crystal growth is epitaxial independent of the orientation of the seed crystal.
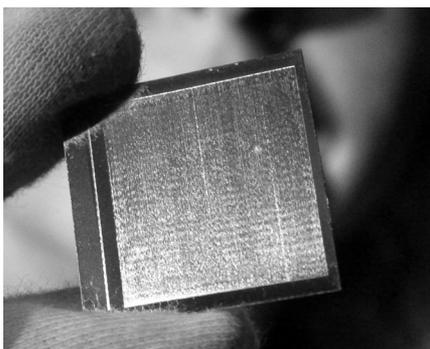


**Figure 2**: 2x2 cm² LLC cell without metallization

Figs. 5 to 7 show I-V-curves of cells with a 700 nm thick seed layer, 2 to 5 µm thick absorber and a 300 nm thick emitter under AM1.5 illumination. The best cells have an open circuit voltage $V_{oc}$ of about 460 mV after remote plasma hydrogen treatment and a short circuit current $I_{sc}$ of 18 mA/cm². Even 510 mV were reached for thinner cells [7].

In Fig. 5 the effect of this passivation treatment is demonstrated for a cell with a 4.5 µm absorber. The hydrogen passivation step increases $V_{oc}$ by more than 100 mV and $I_{sc}$ in the particular case of Fig. 5 from 11 to 15 mA/cm². Fig. 6 shows the influence of the absorber thickness on hydrogen passivated cells.
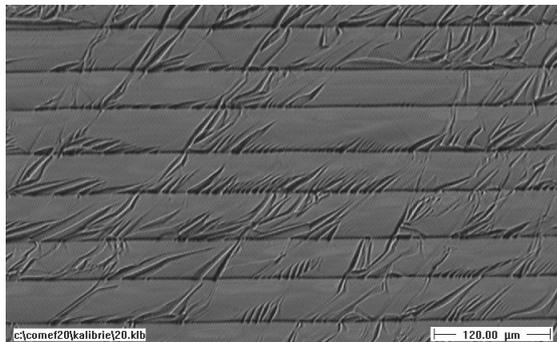


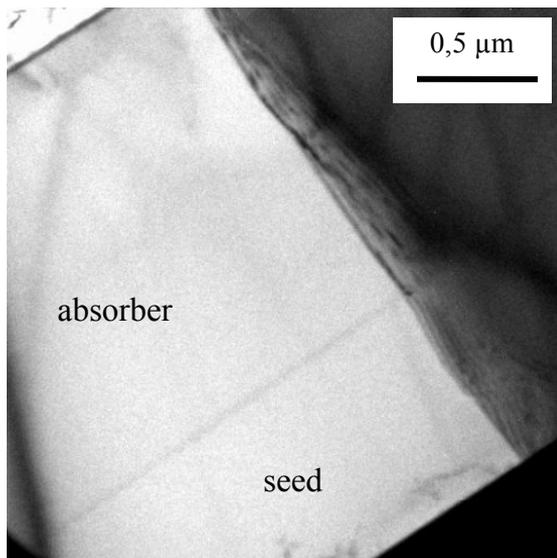**Figure 3**: Optical micrograph of a LLC layer system



**Figure 4**: TEM cross section image of a LLC layer system demonstrating epitaxial growth of the absorber

In order to separate the effects of the crystal quality from those of problems with the contact metallization, in Figs. 5 and 6 the contacting at the seed as well as at the emitter was performed by metal tips. To reduce the series resistance due to the tip contacting only 1 mm² cells were investigated in this case. As expected the short circuit current increases with absorber thickness. However, there is a tendency for lower voltage. This might be due to an increase of defect density during epitaxial thickening. In our cell concept (see Fig. 1) emitter deposition is the last step, so that the p-n-junction is in the region of highest defect concentration.

Another very plausible explanation for the decrease of $V_{oc}$ with increasing thickness is based on the ratio of bulk life time and surface recombination velocity. The $p^+/p$ junction at the seed/absorber interface yields a low effective surface recombination velocity. Combined with

a relatively small bulk life time, saturation current density decreases, and therefore $V_{oc}$ increases with decreasing thickness.
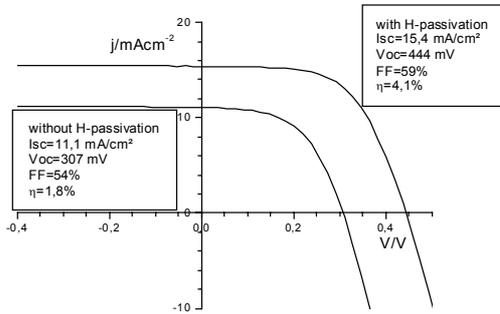


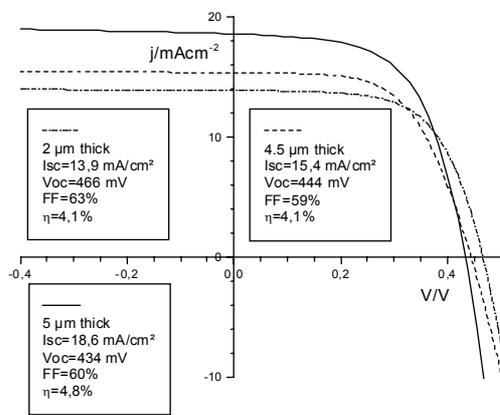**Figure 5**: Effect of hydrogen passivation on a LLC cell with 4.5 µm thick absorber



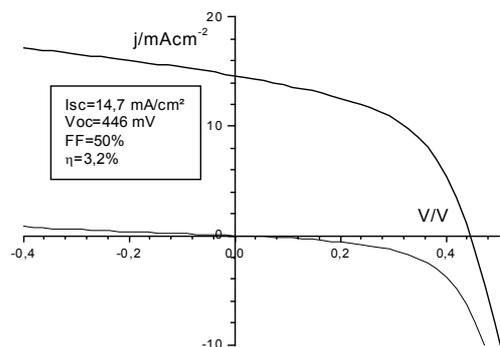**Figure 6**: Effect of absorber thickness on hydrogen passivated LLC cells



**Figure 7**: I-V-curves (dark and illuminated) of a 2.5 µm thick LLC cell 12 mm² in area with TiPdAg metal contact on emitter

Fig. 7 shows the I-V-curve of a 12 mm² cell with 2.5 µm thick absorber, aluminum metallization for seed contacting, and TiPdAg layer as emitter contact. Whereas the cells contacted by tips have low shunting, shunting in the metallized cells is higher leading to a lower fill

factor. Moreover, the TiPdAg layer yields an only moderate reflectivity so that the current is only slightly higher than in bare cells of the same thickness. Experiments to increase reflectivity by Ag metallization were not successful. When we removed the oxide layer on the emitter before metallization the open circuit voltage broke down. If Ag was deposited on top of the oxide, there was no shunting but fill factor and current were low [7] due to high series resistance. Contacting the emitter by an aluminum layer always led to short circuiting.

To assess the potential of the LLC cells and to optimize various process parameters 1-dimensional simulations were performed using PC1D. In order to get relevant input parameters the carrier lifetime in 2x2 cm² cells with a 2 µm thick absorber layer was measured using the MWPCD (Fig. 8) and the QSSPC techniques. With the MWPCD method typical values of 2 µs were determined with some inhomogeneous distribution across the sample, the reason of which is unclear. However, transients with a non-exponential behavior were observed. Hence, the fits to the transients and the derived carrier lifetimes are somehow related to the fit range. We attribute the measured shape of the transients to the structure of the sample. This is confirmed by preliminary PC1D calculations. Nevertheless, the active cell area is clearly visible in the MWPCD scans. However, further investigations and calculations are required for more accurate estimations of the carrier lifetimes within the LLC structure.
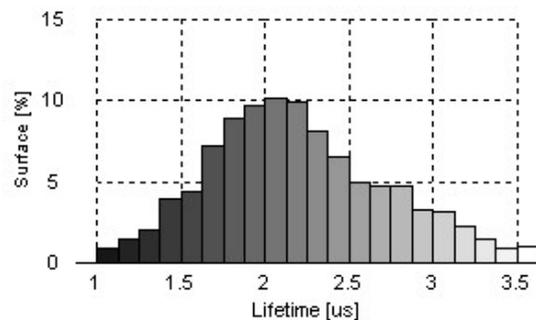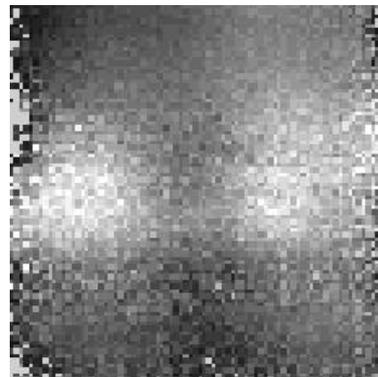


**Figure 8:** MWPCD image of the carrier lifetime (upper part) and corresponding histogram (lower part) of a 2x2 cm² large LLC sample without contacts. The sample is composed of a 0.7 µm thick seed, a 2 µm thick absorber and a 0.3 µm thick emitter layer.

With the QSSPC method, carrier lifetimes of only several ns were determined. These relatively low values

did not match the assumed carrier lifetime in the absorber layer necessary for realistic cell simulations presented below. In addition to that, the measurement is heavily affected by noise. In contrast to cell results, an appreciable increase in the carrier lifetime after hydrogen passivation could be observed by neither carrier lifetime measurement technique.

Table I summarizes measured cell parameters for two cells having an absorber thickness of 2 μm and one cell with an absorber thickness of 5 μm. As can be seen, $V_{oc}$ values as large as 500 mV have been achieved using the LLC concept. If the absorber thickness is increased, the short-circuit current density increases from about 14 mA/cm² to 19 mA/cm². The relatively low fill factors can partly be attributed to high saturation current densities associated with a low open-circuit voltage and partly to a non-optimum contact design. Also included in Table I are simulation results performed using PC1D. For the simulations a 0.7 μm thick p-type seed layer with a doping concentration of $5 \times 10^{19}$ cm$^{-3}$, a p-type absorber layer ($10^{17}$ cm$^{-3}$) and a 0.3 μm thick n-type emitter layer ($5 \times 10^{19}$ cm$^{-3}$) were assumed. The illumination was assumed to be from the seed layer side with a fixed front surface reflectance of 23 %. For the sake of simplicity, no surface recombination velocities were included unless otherwise stated. Furthermore, a series resistance of 3 $\Omega$cm$^2$ was assumed. For the calculations, the carrier lifetime in the absorber layer $\tau$ and in the emitter layer $\tau_e$ and the absorber thickness were varied. As can be seen in Table I, the short-circuit current of a typical LLC-cell can be obtained assuming an absorber lifetime of $\tau = 5$ ns and a 2 μm thick absorber layer. However, the calculated open-circuit voltage is relatively high. In addition to that, the short circuit current decreases to 9.1 mA/cm$^2$ if a thicker absorber is assumed. It can be concluded that the carrier lifetime, or alternatively the diffusion length in the absorber, has to be higher since the collecting junction is at the rear of the cell. For a carrier lifetime of 2 μs the short circuit current increases with absorber thickness. However, at the same time, the open-circuit voltage increases to values in excess of 600 mV. Realistic values of the open-circuit voltages can be achieved by adjusting the emitter quality. Assuming a carrier lifetime in the emitter of 5 ps and an interface recombination velocity between the absorber and the emitter of $10^7$ cm/s, realistic $V_{oc}$ values of about 500 mV are obtained. It can be concluded, that emitter and space charge region quality are critical parameters in the processed LLC-cells.

**Table I**: Measured and simulated cell parameters

| | Cell#/ life time | Abs. thick-ness | $j_{sc}$ mA/cm² | $V_{oc}$ mV | FF % | η % |
|---|---|---|---|---|---|---|
| Exp | H349 | 2 μm | 13.9 | 464 | 62 | 4.0 |
| | X276 | 2 μm | 12.0 | 510 | 30 | 1.6 |
| | H248 | 5 μm | 18.6 | 434 | 60 | 4.8 |
| Sim | $\tau$=5 ns | 2 μm | 14.2 | 525 | 66 | 4.9 |
| | | 5 μm | 9.1 | 506 | 67 | 3.1 |
| | $\tau$=2 μs | 2 μm | 17.1 | 644 | 76 | 8.4 |
| | | 5 μm | 20.5 | 646 | 75 | 9.9 |
| | $\tau$=2 μs | 2 μm | 16.4 | 496 | 71 | 5.8 |
| | $\tau_e$=5 ps | 5 μm | 20.1 | 501 | 70 | 7.0 |

## 4 SUMMARY

Using the LLC process silicon thin film solar cells with an up to 5 μm thick absorber were prepared showing a conversion efficiency of up to 4.8%. Thin cells show an open circuit voltage of up to 510 mV. Increasing the cell thickness leads to a higher current combined with a tendency to lower voltage. These values were achieved with hydrogen passivation by remote microwave plasma treatment. Cell simulations indicate that the short circuit currents correspond to the absorber thickness and to the reflectivity values if a carrier lifetime of several μs in the absorber as measured by MWPCD and several ps in the emitter are assumed together with a interface recombination velocity of $10^7$ cm/s. Emitter and space charge region quality seem to be crucial issues.

To increase the current a light trapping scheme in addition to a metal reflector has to be used. Since we observed short circuiting after metallization the next step will be to introduce a ZnO intermediate layer.

To obtain a high voltage and a high current simultaneously, efficient light trapping is more promising than further increasing the absorber thickness. An alternative could be a cell concept with the p-n-junction located near the seed layer where defect density is lower.

## 5 ACKNOWLEDGEMENT

## 6 REFERENCES

[1]  K. Yamamoto et al., Solar Energy 77 (2004), 939.
[2]  T. Repmann, W. Appenzeller, B. Sehrbrock, H. Stiebig, B. Rech, Proc. 19th Europ. Photovoltaic Solar Energy Conf., Vol. II (2004), 1334.
[3]  R. Brendel, K. Feldrapp, R. Horbelt, R. Auer, phys. stat. sol. (a) 197 (2003), 497.
[4]  J.H. Werner et al., Proc. 3rd World Conf. Photovoltaic Energy Conversion, 2003, 1272.
[5]  A.G. Aberle, A. Straub, P.I. Widenborg, A. Sproul, Y. Huang, P. Campbell, Prog. Photovoltaics 13 (2005), 37.
[6]  G. Andrä, J. Bergmann, F. Falk, E. Ose, 3rd World Conf. Photovoltaic Energy Conversion, Proc. CD (2003), Paper 4P-B4-04G.
[7]  G. Andrä, J. Bergmann, F. Falk, E. Ose, Proc. 19th Europ. Photovoltaic Solar Energy Conf., Vol. I (2004), 873.
[8]  M. Kunst, G. Beck, J. Appl. Phys. 63 (1988), 1093.
[9]  R.A. Sinton, A. Cuevas, Appl. Phys. Lett. 69 (1996), 2510.
[10]  D.A. Clugston, P.A. Basore, Conf. record 26th IEEE PVSC (1997), 207.